

Transport Processes in Metal-Insulator Granular Layers

Yu.G. Pogorelov ^{*}and J. F. Polido

October 29, 2018

CFP/Departamento de Física, Faculdade de Ciências, Universidade do Porto,
Rua do Campo Alegre, 687, 4169-007 Porto, Portugal

Abstract

The non-equilibrium tunnel transport processes are considered in a square lattice of metallic nanogranules embedded into insulating host. Based on a simple model with three possible charging states (\pm , or 0) of a granule and three kinetic processes (creation or recombination of a \pm pair, and charge translation) between neighbor granules, the mean-field kinetic theory is developed, which takes account of the interplay between charging energy and temperature and between the applied electric field and the Coulomb fields by non-compensated charge density. The resulting charge and current distributions are found to depend essentially on the particular conditions in a granular layer, namely, in a free area (FA) or in contact areas (CA) under macroscopic metallic contacts. Thus, a steady state dc transport is only compatible with zero charge density and ohmic resistivity within FA, but charge accumulation and non-ohmic behavior are *necessary* for conduction over CA. The approximate analytic solutions are obtained for characteristic regimes (low or high charge density) of such conduction. Also non-stationary processes are considered, displaying a peculiar combination of two strongly different relaxation times. The comparison is done with the available transport data on similar experimental systems.

PACS: 73.40.Gk, 73.50.-h, 73.61.-r

1 Introduction

Granular (including nanogranular) systems are of a considerable interest for modern technology due to their new physical properties, like giant magnetoresistance [1], Coulomb blockade [2],[3] or high density magnetic memory [4], impossible for classical materials. The systems of our interest here are composed

^{*}Author to whom correspondence should be addressed

from nanoscopic (spherical) metallic particles embedded into insulating matrix, and various existing experimental techniques result in ordered or disordered, mono- or polydispersed, single- or multilayered structures [5]. They are of no less interest from the point of view of fundamental study. In particular, transport phenomena in granular systems reveal certain characteristics which cannot be obtained neither in classical flow regime (in metallic, electrolyte, or gas discharge conduction) nor in hopping regime (in doped semiconductors or in common tunnel junctions). Their specifics is mainly determined by the drastic difference between the characteristic time of an individual tunneling event ($\sim \hbar/\varepsilon_F \sim 10^{-15}$ s) and the interval between such events on the same granule ($\sim e/(jd^2) \sim 10^{-3}$ s, at typical current density $j \sim 10^{-3}$ A/cm² and granule diameter $d \sim 5$ nm). Other important moments are the sizeable Coulomb charging energy $E_c \sim e^2/\varepsilon_{eff}d$ (typically ~ 10 meV) and the fact that the tunneling rates across the layer may be even several orders of magnitude slower than along it. The interplay of all these factors leads to unusual macroscopic effects, thus, a peculiar slow relaxation of electric charge was recently discovered in experiments on tunnel conduction through granular layers and granular films [6],[7]. For theoretical description of such processes we use the model of a single layer of identical spherical particles located in sites of a simple square lattice, with three possible charging states (\pm , or 0) of a granule and three kinetic processes (creation or recombination of a \pm pair, and charge translation) between neighbor granules, and even such simple model reveals a variety of possible dynamical and thermodynamical regimes, to be presented below.

The detailed formulation of the model, its basic parameters, and its mean-field continuum version are given in Sec. 2. Next in Sec. 3 we calculate the mean values of occupation numbers of each charging state for steady state conditions, including the simplest equilibrium situation (no applied fields), in function of temperature. The analysis of current density and related kinetic equation in the out-of-equilibrium case is developed in Sec. 4, where also its simple solution is discussed for the FA part of the system. The most non-trivial regimes are found for the CA part, as described in Sec. 5 for steady state conduction with charge accumulation and non-ohmic behavior. At least, some non-stationary solutions are considered in Sec. 6, either obtained straightforwardly from the time-dependent kinetic equation or estimated from a simplified equivalent circuit. The general integration scheme for non-linear differential equation, corresponding to steady state in CA, and the particular approximations leading to its analytic solutions are dropped into Appendix.

2 Charging states and kinetic processes

We consider a system of identical spherical metallic nanogranules of diameter d , located in sites of simple square lattice of period a within a layer of thickness $b \sim a$ of insulating host with dielectric constant ε (Fig. 1). In the charge transfer processes, granules can bear different numbers σ of electrons in excess (or deficit) to the constant number of positive ions, so that the resulting excess charge σe

defines a certain Coulomb charging energy E_c . At low enough temperatures, which are implied in what follows, the consideration can be limited, besides the ground neutral state $\sigma = 0$, only to single charged states $\sigma = \pm 1$. For the latter case, E_c was given in the classic paper by Sheng and Abeles [8] in the form $E_c = e^2 f(s/d)/(\varepsilon d)$, where s is the mean spacing between granules and the dimensionless function $f(z)$ was estimated for a 3D granular array as $f(z) = 1/(1 + 1/2z)$. Otherwise, the mutual dielectric response of 3D insulating host ($\varepsilon_h = \varepsilon$) with volume fraction $f < 1$ of metallic particles ($\varepsilon_m \rightarrow \infty$) can be characterized by an effective value $\varepsilon_{eff} = \varepsilon/(1 - f)$. For the planar lattice of granules, this effective constant can be estimated, summing the own energy $e^2/\varepsilon d$ of a charged granule at site 0 with the energy of its interaction with electric dipolar moments $\approx (e/\varepsilon_{eff})(d/2n)^3 \mathbf{n}$, induced in each granule at site $\mathbf{n} = a(n_1, n_2)$:

$$E_c = \frac{e^2}{d} \left[\frac{1}{\varepsilon} - \frac{\alpha}{\varepsilon_{eff}} \left(\frac{d}{a} \right)^4 \right] = \frac{e^2}{\varepsilon_{eff} d}. \quad (1)$$

Here the constant $\alpha = (a^4/8) \sum_{\mathbf{n} \neq 0} n^{-4} \approx 0.92$, and the resulting $\varepsilon_{eff} = \varepsilon(1 + \alpha(d/a)^4)$. However, Eq. 1 may underestimate considerably the most important screening from nearest neighbor granules at $d \rightarrow a$, and in what follows we generally characterize the composite of insulating matrix and metallic granules by a certain $\varepsilon_{eff} = e^2/dE_c \gg \varepsilon$.

Following the approach proposed earlier [6], we classify the microscopic states of our system, attributing the charging variable $\sigma_{\mathbf{n}}$ with values ± 1 or 0 to each site \mathbf{n} and then considering three types of kinetic processes between two neighbor granules \mathbf{n} and $\mathbf{n} + \Delta$ (Fig. 2):

1) electron hopping from neutral \mathbf{n} to neutral $\mathbf{n} + \Delta$, creating a pair of oppositely charged granules: $(\sigma_{\mathbf{n}} = 0, \sigma_{\mathbf{n}+\Delta} = 0) \rightarrow (\sigma_{\mathbf{n}} = -1, \sigma_{\mathbf{n}+\Delta} = 1)$, it is only this process that was included in Sheng and Abeles' theory;

2) hopping of an extra electron (hole) from \mathbf{n} to neutral $\mathbf{n} + \Delta$, that is charge transfer: $(\sigma_{\mathbf{n}} = 1, \sigma_{\mathbf{n}+\Delta} = 0) \rightarrow (\sigma_{\mathbf{n}} = 0, \sigma_{\mathbf{n}+\Delta} = 1)$, or $(\sigma_{\mathbf{n}} = -1, \sigma_{\mathbf{n}+\Delta} = 0) \rightarrow (\sigma_{\mathbf{n}} = 0, \sigma_{\mathbf{n}+\Delta} = -1)$;

3) an inverse process to 1), that is recombination of a pair: $(\sigma_{\mathbf{n}} = 1, \sigma_{\mathbf{n}+\Delta} = -1) \rightarrow (\sigma_{\mathbf{n}} = 0, \sigma_{\mathbf{n}+\Delta} = 0)$.

Note that all the processes 1) to 3) are conserving the total system charge $Q = \sum_{\mathbf{n}} \sigma_{\mathbf{n}}$, hence the possibility for charge accumulation or relaxation only appears due to current leads. A typical configuration for current-in-plane (CIP) tunneling conduction includes two macroscopic metallic electrodes on top of the granular layer, forming contact areas (CA) where the current is being distributed from the electrodes into granules through an insulating spacer of thickness b' , and a free area (FA) where the current propagates between the contacts (Fig. 3). To begin with, let us consider a simpler case of FA while the specific analysis for CA with an account for screening effects by metallic contacts will be given later in Sec. 5.

The respective transition rates q_i for the processes 1) to 3) are determined either by the instantaneous charging states of two relevant granules and by the

local electric field $\mathbf{F}_{\mathbf{n}}$ and temperature T , accordingly to the expressions:

$$\begin{aligned} q_{\mathbf{n},\Delta}^{(1)} &= (1 - \sigma_{\mathbf{n}}^2) (1 - \sigma_{\mathbf{n}+\Delta}^2) \varphi(e\mathbf{F}_{\mathbf{n}} \cdot \Delta + E_c), \\ q_{\mathbf{n},\Delta}^{(2)} &= \sigma_{\mathbf{n}}^2 (1 - \sigma_{\mathbf{n}+\Delta}^2) \varphi(-e\mathbf{F}_{\mathbf{n}} \cdot \Delta), \\ q_{\mathbf{n},\Delta}^{(3)} &= \frac{\sigma_{\mathbf{n}}\sigma_{\mathbf{n}+\Delta}(\sigma_{\mathbf{n}}\sigma_{\mathbf{n}+\Delta} - 1)}{2} \varphi(e\sigma_{\mathbf{n}+\Delta}\mathbf{F}_{\mathbf{n}} \cdot \Delta - E_c). \end{aligned} \quad (2)$$

Here the charging energy is taken positive, E_c , for pair creation, zero for transport, and negative, $-E_c$, for recombination. The function $\varphi(E) = \omega N_{\mathbf{F}} E / (e^{\beta E} - 1)$ expresses the total probability, at given $\beta = 1/k_{\mathbf{B}}T$, for electron transition between granules with Fermi density of states $N_{\mathbf{F}}$ and Fermi levels differing by E . The hopping frequency $\omega = \omega_a e^{-2\chi s}$ is expressed through the “attempt” frequency $\omega_a \sim \varepsilon_{\mathbf{F}}/\hbar$, the inverse tunneling length χ (typically $\sim 10 \text{ nm}^{-1}$), and the intergranule spacing $s = a - d$. Local electric field $\mathbf{F}_{\mathbf{n}}$ on \mathbf{n} th site consists of the external field \mathbf{F}_{ext} and the Coulomb field $\mathbf{F}_{\mathbf{n}}^{Coul}$ due to all other charged granules (from FA):

$$\mathbf{F}_{\mathbf{n}}^{Coul} = \frac{e}{\varepsilon_{eff}} \sum_{\mathbf{n}' \neq \mathbf{n}} \sigma_{\mathbf{n}'} \frac{\mathbf{n}' - \mathbf{n}}{|\mathbf{n}' - \mathbf{n}|^3}. \quad (3)$$

A suitable approximation for such a system is achieved with passing from discrete-valued functions $\sigma_{\mathbf{n}}$ of discrete argument $\mathbf{n} = a(n_1, n_2)$ to their continuous-valued mean-field (MF) equivalents $\sigma(\mathbf{r}) = \langle \sigma_{\mathbf{n}} \rangle_{\mathbf{r}}$ (mean charge density) and $\rho(\mathbf{r}) = \langle \sigma_{\mathbf{n}}^2 \rangle_{\mathbf{r}}$ (mean charge carrier density), obtained by averaging over a wide enough (that is, great compared to the lattice period but small compared to the size of entire system or its parts) area around \mathbf{r} , the latter being *any* point in the plane. This also implies passing to smooth local field:

$$\mathbf{F}(\mathbf{r}) = \mathbf{F}_{ext} + \frac{e}{\varepsilon_{eff}a^2} \int \sigma(\mathbf{r}') \frac{\mathbf{r}' - \mathbf{r}}{|\mathbf{r}' - \mathbf{r}|^3} d\mathbf{r}'. \quad (4)$$

and to averaged transition rates $q^{(i)}(\mathbf{r}, \Delta) = \langle q_{\mathbf{n},\Delta}^{(i)} \rangle_{\mathbf{r}}$ and $p^{(i)}(\mathbf{r}, \Delta) = \langle \sigma_{\mathbf{n}} q_{\mathbf{n},\Delta}^{(i)} \rangle_{\mathbf{r}}$. These rates just define the temporal evolution of mean densities:

$$\begin{aligned} \dot{\sigma}(\mathbf{r}) &= \sum_{\Delta} \left[q^{(1)}(\mathbf{r}, \Delta) - q^{(1)}(\mathbf{r} + \Delta, -\Delta) - p^{(2)}(\mathbf{r}, \Delta) + \right. \\ &\quad \left. + p^{(2)}(\mathbf{r} + \Delta, -\Delta) - p^{(3)}(\mathbf{r}, \Delta) \right], \end{aligned} \quad (5)$$

$$\begin{aligned} \dot{\rho}(\mathbf{r}) &= \sum_{\Delta} \left[q^{(1)}(\mathbf{r}, \Delta) + q^{(1)}(\mathbf{r} + \Delta, -\Delta) - q^{(2)}(\mathbf{r}, \Delta) + \right. \\ &\quad \left. + q^{(2)}(\mathbf{r} + \Delta, -\Delta) - q^{(3)}(\mathbf{r}, \Delta) \right]. \end{aligned} \quad (6)$$

The set of Eqs. 2-6 is complete to provide a continuous description of the considered system, once a proper averaging procedure is established.

3 Mean-field densities in equilibrium

We perform the above defined averages in the simplest assumption of no correlations between different sites: $\langle f_{\mathbf{n}} g_{\mathbf{n}'} \rangle = \langle f_{\mathbf{n}} \rangle \langle g_{\mathbf{n}'} \rangle$, $\mathbf{n}' \neq \mathbf{n}$, and using the evident rules: $\langle \sigma_{\mathbf{n}}^{2k+1} \rangle_{\mathbf{r}} = \sigma(\mathbf{r})$, $\langle \sigma_{\mathbf{n}}^{2k} \rangle_{\mathbf{r}} = \rho(\mathbf{r})$. The resulting averaged rates are:

$$\begin{aligned}
q^{(1)}(\mathbf{r}, \Delta) &= \sigma^0(\mathbf{r}) \sigma^0(\mathbf{r} + \Delta) \varphi [e\mathbf{F}(\mathbf{r}) \cdot \Delta + E_c], \\
q^{(2)}(\mathbf{r}, \Delta) &= \sigma^0(\mathbf{r} + \Delta) \{ \sigma^+(\mathbf{r}) \varphi [-e\mathbf{F}(\mathbf{r}) \cdot \Delta] + \sigma^-(\mathbf{r}) \varphi [e\mathbf{F}(\mathbf{r}) \cdot \Delta] \}, \\
p^{(2)}(\mathbf{r}, \Delta) &= \sigma^0(\mathbf{r} + \Delta) \{ \sigma^+(\mathbf{r}) \varphi [-e\mathbf{F}(\mathbf{r}) \cdot \Delta] - \sigma^-(\mathbf{r}) \varphi [e\mathbf{F}(\mathbf{r}) \cdot \Delta] \}, \\
q^{(3)}(\mathbf{r}, \Delta) &= \{ \sigma^-(\mathbf{r}) \sigma^+(\mathbf{r} + \Delta) \varphi [e\mathbf{F}(\mathbf{r}) \cdot \Delta - E_c] + \\
&\quad + \sigma^+(\mathbf{r}) \sigma^-(\mathbf{r} + \Delta) \varphi [-e\mathbf{F}(\mathbf{r}) \cdot \Delta - E_c] \}, \\
p^{(3)}(\mathbf{r}, \Delta) &= \{ \sigma^-(\mathbf{r}) \sigma^+(\mathbf{r} + \Delta) \varphi [e\mathbf{F}(\mathbf{r}) \cdot \Delta - E_c] - \\
&\quad - \sigma^+(\mathbf{r}) \sigma^-(\mathbf{r} + \Delta) \varphi [-e\mathbf{F}(\mathbf{r}) \cdot \Delta - E_c] \},
\end{aligned} \tag{7}$$

where the mean occupation numbers for each charging state $\sigma^\pm(\mathbf{r}) = [\rho(\mathbf{r}) \pm \sigma(\mathbf{r})]/2$ and $\sigma^0(\mathbf{r}) = 1 - \rho(\mathbf{r})$ satisfy the normalization condition: $\sum_i \sigma^i(\mathbf{r}) = 1$.

In a similar way to Eq. 5, we express the vector of average current density $\mathbf{j}(n)$ at \mathbf{n} th site:

$$\begin{aligned}
\mathbf{j}(n) &= \frac{e}{a^2 b} \sum_{\Delta} \Delta \left[-q^{(1)}(\mathbf{n}, \Delta) + q^{(1)}(\mathbf{n} + \Delta, -\Delta) + p^{(2)}(\mathbf{n}, \Delta) - \right. \\
&\quad \left. - p^{(2)}(\mathbf{n} + \Delta, -\Delta) + p^{(3)}(\mathbf{n}, \Delta) \right],
\end{aligned} \tag{8}$$

then its MF extension $\mathbf{j}(r)$ is obtained by simple replacing \mathbf{n} by \mathbf{r} in the arguments of $q^{(i)}$ and $p^{(i)}$. Expanding these continuous functions in powers of $|\Delta| = a$, we conclude that Eq. 5 reduces to usual continuity equation:

$$\dot{\sigma}(\mathbf{r}) = -\frac{a^2 b}{e} \nabla_2 \cdot \mathbf{j}(r), \tag{9}$$

with the 2D nabla: $\nabla_2 = (\partial/\partial x, \partial/\partial y)$.

We begin the analysis of Eqs. 5-9 from the simplest situation of thermal equilibrium in absence of electric field, $\mathbf{F}(r) \equiv 0$, then Eq. 5 turns into evident identity: $\sigma(\mathbf{r}) \equiv 0$, that means zero charge density, and Eq. 8 yields in zero current density: $\mathbf{j}(r) \equiv 0$, while Eq. 6 provides a finite and constant value of charge carrier density:

$$\rho(\mathbf{r}) \equiv \rho_0 = \frac{2}{2 + \exp(\beta E_c/2)}. \tag{10}$$

At low temperatures, $\beta E_c \gg 1$, this value is exponentially small: $\rho_0 \approx 2 \exp(-\beta E_c/2)$, and for high temperatures, $\beta E_c \ll 1$, it tends as $\rho_0 \approx \rho_\infty - \beta E_c/9$ to the limit $\rho_\infty = 2/3$, corresponding to equipartition between all three fractions σ^i (Fig. 4).

In presence of electric fields $\mathbf{F}(r) \neq 0$, the local equilibrium should be perturbed and the system can generate current and possibly accumulate charge. Our further analysis is aimed to demonstrate that the latter process is impossible in FA, but, supposing for a moment a non-zero charge density $\sigma(\mathbf{r})$, we obtain from Eq. 6 a more general local relation between $\sigma(\mathbf{r})$ and $\rho(\mathbf{r})$:

$$\sigma^2(\mathbf{r}) = \frac{[\rho(\mathbf{r}) - \rho_0][\rho(\mathbf{r}) + \rho_0 - 2\rho_0\rho(\mathbf{r})]}{1 - \rho_0}, \quad (11)$$

describing the increase of charge density with going away from equilibrium (Fig. 5). Now we are in position to pass to the out-of-equilibrium situations, beginning from a simpler case of dc current flowing through FA.

4 Steady state conduction in FA

In presence of (generally non-uniform) fields $\mathbf{F}(r)$ and densities $\sigma(\mathbf{r})$, $\rho(\mathbf{r})$, we expand Eq. 8 up to 1st order terms in $|\Delta| = a$ and obtain the local current density as a sum of two contributions, field-driven and diffusive:

$$\mathbf{j}(r) = \mathbf{j}_{field}(\mathbf{r}) + \mathbf{j}_{dif}(\mathbf{r}) = G[\rho(\mathbf{r})]\mathbf{F}(r) - eD[\rho(\mathbf{r})]\nabla_2\sigma(\mathbf{r}), \quad (12)$$

where the effective conductivity G and diffusion coefficient D are functions of local charge carrier density ρ :

$$G(\rho) = \frac{4e^2(1-\rho)}{a} |\rho\varphi'(0) + 2(1-\rho)\varphi'(E_c) + \beta\varphi(E_c)|, \quad (13)$$

$$D(\rho) = \frac{(1-\rho)[\rho\varphi(0) - 2(1-\rho)\varphi(E_c)]}{a(\rho - \sigma^2)}. \quad (14)$$

Note that $\rho - \sigma^2$ in Eq. 14 is nothing but the mean square dispersion of charge density, and it is expressed through ρ by Eq. 11. In view of this equation, we can also consider G and D as *even* functions of local charge density σ , and just this dependence will be mostly used below. Also G and D depend on temperature, through the functions φ , φ' . The system of Eqs. 11-14, together with Eq. 4, is closed and self-consistent, defining the distributions of $\sigma(\mathbf{r})$ and $\rho(\mathbf{r})$ at given $\mathbf{j}(r)$.

Substituting Eq. 12 into Eq. 9 and considering the low temperature limit when the diffusion coefficient D is practically independent of σ , we transform the kinetic equation to the form:

$$\dot{\sigma} - a^2bD\Delta_2\sigma = -\frac{a^2b}{e}\nabla_2[G(\sigma)\mathbf{F}]. \quad (15)$$

where the l.h.s. has an aspect of common 2D diffusion equation and the r.h.s. plays the role of source (or drain) function. For the FA case, with the local field \mathbf{F} defined by Eq. 4 and the only relevant coordinate being x , along the current

$\mathbf{j}(r) = \text{const}$ (Fig. 3), Eq. 15 under steady state condition ($\dot{\sigma} = 0$) leads to a (non-linear) integral equation for $\sigma(x)$:

$$\sigma(x) = \frac{1}{eD} \int_0^x \left\{ G[\sigma(x')] \left[\mathbf{F}_{ext} + \frac{e}{\varepsilon_{eff} a^2} \int_{-L/2}^{L/2} \frac{\sigma(x'')}{x' - x''} dx'' \right] - j \right\} dx'. \quad (16)$$

Numeric analysis of Eq. 16 shows that there is no other its solution but the trivial one: $\sigma(\mathbf{r}) \equiv 0$. Hence there is no diffusive contribution to the current, and the steady state of FA in out-of-equilibrium conditions has an ohmic resistivity:

$$r = \frac{1}{G(\rho_0)}. \quad (17)$$

With the parameter values $a \sim 5$ nm, $\omega \sim 10^{12}$ s $^{-1}$, $N_F \sim 1$ eV $^{-1}$, $E_c \sim 10$ meV, $T \sim 12$ K, used in Eqs. 13, 11, we have $r \sim 50$ Ω cm, which is in a reasonable agreement with the measured resistance $R \sim 50 \div 100$ M Ω in a 10 layer granular sample of $\sim 1 \times 1$ cm area [6].

5 Steady state conduction in CA

The kinetics in CA includes, besides the processes 1) to 3) of Sec. 3, also 4 additional microscopic processes between n th granule and the electrode (Fig. 6) which are just responsible for variations of total charge Q by ± 1 . The respective rates $q^{(i)}$, $i = 4, \dots, 7$, are also dependent on the charging state (σ, ρ) of the relevant granule and, using the same techniques that before for FA, we obtain their mean values as:

$$\begin{aligned} q^{(4)} &= (\rho + \sigma) \psi(-U - E'_c), & q^{(5)} &= (\rho - \sigma) \psi(U - E'_c), \\ q^{(6)} &= (1 - \rho) \psi(U + E'_c), & q^{(7)} &= (1 - \rho) \psi(-U + E'_c). \end{aligned} \quad (18)$$

Here the function $\psi(E)$ formally differs from $\varphi(E)$ only by changing the prefactor: $\omega \rightarrow \omega' = \omega_a e^{-2\chi b'} \ll \omega$, but the arguments of these functions in Eq. 18 include other characteristic energies. Thus, $U = eb'F_c$ is generated by the electric field F_c between granule and contact surface. This field is always normal to the surface (see Fig. 7) and its value is defined by the local charge density σ . At least, the charging energy E'_c for a granule under the contact can be somewhat reduced (e.g., by $\sim 1/2$) compared to E_c . Then the kinetic equations in CA present a generalization of Eqs. 5,6, as follows:

$$\begin{aligned} \dot{\sigma}(\mathbf{r}) &= \sum_{\Delta} \left[q^{(1)}(\mathbf{r}, \Delta) - q^{(1)}(\mathbf{r} + \Delta, -\Delta) - p^{(2)}(\mathbf{r}, \Delta) + \right. \\ &\quad \left. + p^{(2)}(\mathbf{r} + \Delta, -\Delta) - p^{(3)}(\mathbf{r}, \Delta) - q^{(4)}(\mathbf{r}) + q^{(5)}(\mathbf{r}) + q^{(6)}(\mathbf{r}) - q^{(7)}(\mathbf{r}) \right], \\ \dot{\rho}(\mathbf{r}) &= \sum_{\Delta} \left[q^{(1)}(\mathbf{r}, \Delta) + q^{(1)}(\mathbf{r} + \Delta, -\Delta) - q^{(2)}(\mathbf{r}, \Delta) + \right. \end{aligned} \quad (19)$$

$$+q^{(2)}(\mathbf{r} + \Delta, -\Delta) - q^{(3)}(\mathbf{r}, \Delta) - q^{(4)}(\mathbf{r}) - q^{(5)}(\mathbf{r}) + q^{(6)}(\mathbf{r}) + q^{(7)}(\mathbf{r}) \Big].$$

The additional terms, by the “normal” processes 4 to 7, are responsible for appearance of a *normal* component of current density:

$$\mathbf{j}_z(\mathbf{r}) = \frac{e\mathbf{b}}{a^2b} \left[q^{(4)}(\mathbf{r}) - q^{(5)}(\mathbf{r}) - q^{(6)}(\mathbf{r}) + q^{(7)}(\mathbf{r}) \right], \quad (20)$$

besides the planar component, still given by Eq. 8. But even more important difference from the FA case consists in the fact that the Coulomb field here is formed by a *double layer* of charges, those of granules themselves and their images in the metallic electrode (Fig. 7). Summing the contributions from all the charged granules and their images (except for the image of n th granule itself, already included in the energy E'_c), we arrive at the expression for the above mentioned field F_c at the contact surface as a *local* function of the charge density $\sigma(\mathbf{r})$:

$$F_c(\mathbf{r}) = F^{Coul}(\mathbf{r}, z = b') = -\frac{4\pi e\sigma(\mathbf{r})}{\varepsilon_{eff}a^2}, \quad (21)$$

(instead of integral relations, Eqs. 3,4, in FA). Then, the planar component of the field by charged granules $\mathbf{F}_{pl}(\mathbf{r}) = \mathbf{F}^{Coul}(\mathbf{r}, z = 0)$ is determined by the above defined normal field F_c through the relation $\mathbf{F}_{pl}(\mathbf{r}) = b'\nabla_2 F_c(\mathbf{r})$. The density of planar current is $\mathbf{j}_{pl}(\mathbf{r}) = G\mathbf{F}_{pl}(\mathbf{r}) - eD\nabla_2\sigma(\mathbf{r})$, accordingly to Eq. 12, that is both field-driven and diffusive contributions into \mathbf{j}_{pl} are present here and both they are proportional to the gradient of $\sigma(\mathbf{r})$. In the low temperature limit, this proportionality is given by:

$$\mathbf{j}_{pl}(\mathbf{r}) \approx -\left\{ \frac{8\pi e^3\omega N_{\mathbf{F}}b'}{\varepsilon_{eff}a^3}g[\sigma(\mathbf{r})] + \frac{e\omega N_{\mathbf{F}}k_{\mathbf{B}}T}{a} \right\} \nabla_2\sigma(\mathbf{r}). \quad (22)$$

Note that presence of a non-linear function:

$$g(\sigma) = \sqrt{\rho_0^2 + \sigma^2} - \rho_0^2 - \sigma^2, \quad (23)$$

defines a *non-ohmic* conduction in CA. In fact, this function should be given by Eq. 23 up to maximum possible charge density $|\sigma_{max}| = \sqrt{1 - \rho_0^2}$, turning zero for $|\sigma| > |\sigma_{max}|$ (note that the latter restriction just corresponds to our initial limitation to the single charged states, see Sec. 2). In the same limit of low temperatures, the normal current density is obtained from Eqs. 18,20 as $\mathbf{j}_z(\mathbf{r}) = G_z\mathbf{F}_c(\mathbf{r})$ where $G_z \approx \omega'N_{\mathbf{F}}E'_c\varepsilon_{eff}/4\pi$. Finally, the kinetic equation in this case is obtained, in analogy with Eq. 9, as:

$$\dot{\sigma}(\mathbf{r}) = -\frac{a^2b}{e}\nabla_2 \cdot \mathbf{j}_{pl}(\mathbf{r}) + \frac{a^2}{e}j_z(\mathbf{r}). \quad (24)$$

This equation permits to describe the steady state conduction as well as various time dependent processes. The first important conclusion is that steady state conduction in CA turns only possible at non-zero charge density gradient, that

is, *necessarily* involving charge accumulation, in contrast to the above considered situation in FA.

Let us begin from the steady state regime which is simpler, in order to use the obtained results later for the analysis of a more involved case when an explicit temporal dependence of charge density is included in Eq. 24.

We choose the CA geometry in the form of a rectangular stripe of planar dimensions $L \times L'$, along and across the current respectively. In neglect of relatively small effects of current non-uniformity along the lateral boundaries, the only relevant coordinate for the problem is longitudinal, x (Fig. 8). In the steady state regime, the temporal derivative $\dot{\sigma}$ in Eq. 24 is zero and the total current $I = \text{const}$, defined by the action of external source. Then, using Eq. 23, we arrive at a non-linear 2nd order equation for charge density:

$$\frac{d}{dx} \{g[\sigma(x)] + \tau\} \frac{d\sigma(x)}{dx} - k^2 \sigma(x) = 0. \quad (25)$$

The parameters in Eq. 25 are: $k^2 = (\omega' E'_c)/(ab\omega k_B T_1)$ and $\tau = T/T_1$, where T is the actual temperature and $T_1 = 8\pi e^2 b'/a^2 b \varepsilon_{eff}$. To define completely its solution, the following boundary conditions are imposed:

$$\left. \frac{d\sigma(x)}{dx} \right|_{x=0} = \frac{k^2 b' \sigma(x=0)}{g[\sigma(0)] + \tau} \quad (26)$$

$$\left. \frac{d\sigma(x)}{dx} \right|_{x=L} = \frac{a}{LewbN_F k_B T_1} \frac{I}{g[\sigma(x=L)] + \tau} \quad (27)$$

The condition 26 corresponds to the fact that the longitudinal current j_x at the initial point of CA (the leftmost in Fig. 8) is fully supplied by the normal current j_y entering from the contact to granular sample, and the condition 27 corresponds to current continuity at passing from CA (of length L along the current) to FA.

Let us discuss the solution of Eq. 25 qualitatively. Generally, to fulfill the conditions, Eqs. 26,27, one needs a quite subtle balance to be maintained between the charge density and its derivatives at both ends of CA. But the situation is radically simplified when the length L is much greater than the characteristic decay length for charge and current density: $kL \gg 1$. In this case, the relevant coordinate is $\xi = L - x$, so that the boundary condition 26 corresponds to $\xi = L \rightarrow \infty$, when both its left and right hand side turn zeros:

$$\sigma(\xi)|_{\xi \rightarrow \infty} = 0, \quad \left. \frac{d\sigma(\xi)}{d\xi} \right|_{\xi \rightarrow \infty} = 0. \quad (28)$$

The numeric solution shows that, for any initial (with respect to ξ , that is related to $x = L$, Eq. 27) value of charge density $\sigma(\xi = 0) = \sigma_0$, there is a *unique* initial value of its derivative $d\sigma(\xi)/d\xi|_{\xi=0} = D(\sigma_0)$ which just assures the limits 28, while for $d\sigma(\xi)/d\xi|_{\xi=0} > D(\sigma_0)$ the asymptotic value diverges as $\sigma(\xi \rightarrow \infty) \rightarrow \infty$, and for $d\sigma(\xi)/d\xi|_{\xi=0} < D(\sigma_0)$ it diverges as $\sigma(\xi \rightarrow \infty) \rightarrow -\infty$. Then, using the boundary condition 27 and taking into account the relation $V = V_0 \sigma_0$

following from Eq. 21 with $V_0 = 4\pi eb'/(\varepsilon_{eff}a^2)$, we conclude that the function $D(\sigma_0)$ generates the I - V characteristics for CA:

$$I = I_1 b' D(V/V_0) [g(V/V_0) + \tau] \quad (29)$$

where $I_1 = e\omega N_F k_B T_1$.

A more detailed analysis of Eq. 25 is presented in Appendix. In particular, for the weak current regime (regime I) when $\sigma_0 \ll \sigma_1 = \sqrt{32\rho_0(\rho_0 + \tau)} \ll 1$, so that $g(\sigma) \approx \rho_0 + \sigma^2/2\rho_0$ along whole CA, Eq. 25 admits an approximate analytic solution:

$$\sigma(\xi) = \sigma_0 e^{-\lambda\xi} \left[1 + 6 \left(\frac{\sigma_0}{\sigma_1} \right)^2 (1 - e^{-2\lambda\xi}) \right], \quad (30)$$

with the exponential decay index $\lambda = k/\sqrt{\rho_0 + \tau}$. This results in the explicit I - V characteristics for regime I:

$$I = \frac{V}{R_0(\tau)} \left[1 + \left(\frac{V}{V_1} \right)^2 \right], \quad (31)$$

presented by the line 1 in Fig. 9. For $V < V_1 = \sigma_1 V_0$, Eq. 31 describes the initial ohmic resistance (dependent on temperature τ):

$$R_0(\tau) = \frac{V_0}{I_1 k b' \sqrt{\rho_0(\tau) + \tau}}, \quad (32)$$

which turns non-ohmic for $V \sim V_1$. But at so high voltages another conduction regime already applies (called regime II), where $\sigma_1 \ll \sigma_0 \ll 1$ and one has $g(\sigma) \approx \sigma$ (see Eq. 23). Following the same reasoning as for the regime I, we obtain a non-linear I - V characteristics for regime II:

$$I \approx \frac{I_1 k b'}{\sqrt{3}} \left(\frac{V}{V_0} + \tau \right)^{3/2}, \quad (33)$$

presented by the line 2 in Fig. 9. This law is weaker temperature dependent than Eq. 31, which relates to the fact that the conductance in regime II is mainly due to dynamical accumulation of charge and not to thermic excitation of charge carriers. However, such dependence can be more pronounced if multiple charging states are engaged, as may be the case in real granular layers with a certain statistical distribution of granule sizes present.

At least, for even stronger currents, when already $\sigma_0 \sim 1$, the solutions of Eq. 25 can be obtained numerically, following the above discussed procedure of adjustment of the derivative $D(\sigma_0)$ to a given σ_0 . Such solutions define the line 3 in Fig. 9, which generally agrees with the lines 1 and 2, but its asymptotics turns to $I \sim V^{5/4}$.

A simple and important exact relation for the total accumulated charge Q in CA is obtained from the direct integration of Eq. 25:

$$Q = \tau I, \quad (34)$$

where the parameter $\tau = 1/\psi(-E'_c)$ has a role of characteristic relaxation time in non-stationary processes, as will be seen below. Assuming its value $\tau \sim 1$ s (comparable with the experimental observations [6]), together with the above used values of ω and T_1 , we conclude that the characteristic length scale λ^{-1} for solutions of Eq. 25 can reach up to $\sim 10^4 a \sim 0.1$ mm, which is a reasonable scale for a charge distribution beneath the contacts.

6 Time-dependent processes

Now we can extend our analysis also to a non-stationary situation. Actually, let us consider the simplest example of this type, that of interrupting the circuit of Fig. 3 at the moment $t_0 = 0$, after an infinitely long steady state with current I . Beginning from this moment, the constant value is not the total current, as was the case in Sec. 3, but the total charge in the overall system composed by the granular sample itself and electrodes (in fact, this total value is zero and it corresponds to the uniform distribution $\sigma(\mathbf{r}, \infty) \equiv 0$ in the asymptotic limit $t \rightarrow \infty$). We use the same 1D geometry and, accordingly to the above mentioned absence of charges in FA, limit ourselves only to consideration of CA. The initial distribution $\sigma(x)$, corresponding to the steady state, will degrade at $t > t_0$, at the expense of recombination of charges accumulated in granules beneath the contact with the polarization charges on the contact surface (the “image” charges). This process is described by Eq. 24, subject to the initial condition $\sigma(x, t = t_0) \equiv 0$ and the boundary conditions:

$$\dot{\sigma}(L, t) = -\frac{\sigma(L, t)}{\tau} + \frac{g[\sigma(x, t)] + \tau}{\tau b k^2} \frac{d\sigma(x, t)}{dx} \Big|_{x=L} + \frac{I - C\dot{V}}{eL'b}, \quad (35)$$

$$\dot{\sigma}(0, t) = -\frac{\sigma(0, t)}{\tau} - \frac{g[\sigma(x, t)] + \tau}{\tau b k^2} \frac{d\sigma(x, t)}{dx} \Big|_{x=0}, \quad (36)$$

where V and C are respectively the voltage and capacitance between the contacts. In similarity with the above considered steady state case, the non-stationary Eq. 24 with the boundary conditions, Eqs. 35,36, can be solved numerically, in fact presenting an exponential decay with characteristic time $\sim \tau$ (the corresponding plot not shown here).

But a more transparent description of dynamical processes in the considered system is achieved with using the equivalent circuit (Fig. 10), following from the previous analysis. Here R represents the resistance of FA, which is ohmic (due to the absence of charges) but strongly temperature dependent. The two resistances R' associated to each CA are already non-ohmic, as seen from Eqs. 22,23, due to the accumulated charge Q . The proportionality between Q and the current I_{CA} through CA, Eq. 34, together with the simplifying assumption of uniform charge distribution over the rectangular CA, permits to express this non-ohmic behavior through the function g given by Eq. 23:

$$R'(I_{CA}) = \frac{R_0}{g(I_{CA}/I_0)}. \quad (37)$$

Here the resistance scale $R_0 = aL/(4bL'e^2\varphi'(0))$ can be fixed by a direct comparison with the experimentally measured steady state resistance of the whole circuit, and the current scale $I_0 = eLL'/(\tau a^2)$ is about $1 \mu\text{A}$ for $L \sim L' \sim 1 \text{ cm}$ and $a \sim 5 \text{ nm}$. The respective capacities have the orders of magnitude: $C_1 \sim L$ (capacity between the electrodes through FA) and $C_2 \sim LL'/b$ (capacity between an electrode and adjacent granular layer), hence $C_1 \ll C_2$. Then the temporal evolution of the system is given by the equations for voltages V_1 and V_2 on them:

$$\begin{aligned}\dot{V}_1 &= \frac{2V_2 - V_1}{RC}, \\ \dot{V}_2 &= \frac{V_1}{RC'} - \left(\frac{2}{RC'} + \frac{g(V_2)}{C'} \right) V_2.\end{aligned}\tag{38}$$

The numeric solution to this equivalent system with initial conditions $V_1(0) = V$, $V_2(0) = (V - IR_1)/2$, adequate to the considered discharge regime, is presented in Fig. 11. It can be noted that the character of decay is very similar to that obtained with the exact kinetic equation, Eq. 24. Another interesting moment is the presence of two “relaxation times” seen in a log plot (lower panel of Fig. 11). The initial discharge phase, with the strongest current through CA and the lowest resistance R' (by Eq. 37), has a very fast decay whereas the final phase has a much slower relaxation rate, due to the growth of R' . This behavior also agrees with the experimental observations at switching off the current through a granular layer [6], revealing two strongly different relaxation times, the faster one being temperature dependent.

The relatively simple non-linear system, Eqs. 38, can be also used for treating more complicate transient processes.

7 Appendix

Let us consider the equation:

$$\frac{d}{d\xi} [g(\sigma) + \tau] \frac{d\sigma}{d\xi} - k^2\sigma = 0\tag{39}$$

with certain boundary conditions $\sigma(0) = \sigma_0$, $\sigma'(0) = \sigma'_0$, resulting from Eqs. 26,27. For a rather general function $g(\sigma)$ we can define the function

$$f(\sigma) = \int_0^\sigma g(\sigma') d\sigma',\tag{40}$$

then Eq. 39 presents itself as:

$$\frac{d^2 F(\xi)}{d\xi^2} = k^2\sigma(\xi),\tag{41}$$

where $F(\xi) \equiv f[\sigma(\xi)] + \tau\sigma(\xi)$. Considered irrespectively of ξ :

$$f(\sigma) + \tau\sigma = F,\tag{42}$$

this equation also defines σ as a certain function of F : $\sigma = \sigma(F)$. Hence it is possible to construct the following function:

$$\varphi(F) = 2 \int_0^F \sigma(F') dF'. \quad (43)$$

Now, multiplying Eq. 41 by $2dF/d\xi$, we arrive at the equation:

$$\frac{d}{d\xi} \left(\frac{dF}{d\xi} \right)^2 = k^2 \frac{d\varphi}{d\xi}, \quad (44)$$

with $\varphi(\xi) \equiv \varphi[F(\xi)]$. Integrating Eq. 44 in ξ , we obtain a 1st order separable equation for $F(\xi)$:

$$\frac{dF}{d\xi} = \pm k \sqrt{\varphi(F)}. \quad (45)$$

We expect the function F to decrease at going from $\xi = 0$ into depth of CA, hence choose the negative sign on r.h.s. of Eq. 45 and obtain its explicit solution as

$$\int_{F(\xi)}^{F_0} \frac{dF'}{\sqrt{\varphi(F')}} = k\xi \quad (46)$$

with $F_0 = f(\sigma_0) + \tau\sigma_0$. Finally, the sought solution for $\sigma(\xi) = \sigma[F(\xi)]$ results from substitution of the function $F(\xi)$, given implicitly by Eq. 46, into $\sigma(F)$ defined by Eq. 42. Consider some particular realizations of the above scheme.

For the function $g(\sigma)$ given by Eq. 23, we have the explicit integral, Eq. 40, in the form:

$$F(\sigma) = f(\sigma) + \tau\sigma = \left(\tau + \frac{\sqrt{\rho_0^2 + \sigma^2}}{2} - \rho_0 - \frac{\sigma^2}{3} \right) \sigma + \rho_0^2 \ln \sqrt{\frac{\sigma + \sqrt{\rho_0^2 + \sigma^2}}{\rho_0}}. \quad (47)$$

In the case $\sigma \ll \rho_0 \ll 1$ (regime I), Eq. 47 is approximated as:

$$F \approx (\rho_0 + \tau) \sigma + \frac{\sigma^3}{6\rho_0} \quad (48)$$

hence $\sigma(F)$ corresponds to a real root of the cubic equation, Eq. 48, and in the same approximation of regime I it is given by:

$$\sigma(F) \approx \frac{F}{\rho_0 + \tau} \left(1 - \frac{8F^2}{\sigma_1^2} \right), \quad (49)$$

with $\sigma_1 = 4\sqrt{\rho_0(\rho_0 + \tau)^3}$. Using this form in Eq. 43, we obtain:

$$\varphi(F) \approx \frac{F^2}{\rho_0 + \tau} \left(1 - \frac{4F^2}{\sigma_1^2} \right), \quad (50)$$

and then substituting into Eq. 46:

$$\ln \frac{\left[1 + \sqrt{1 - (2F/\sigma_1)^2}\right] F_0}{\left[1 + \sqrt{1 - (2F_0/\sigma_1)^2}\right] F} = \lambda \xi. \quad (51)$$

Inverting this relation, we define an explicit solution for $F(\xi)$:

$$F(\xi) \approx F_0 e^{-\lambda \xi} \left[1 + \frac{F_0^2}{\sigma_1^2} (1 - e^{-2\lambda \xi})\right]. \quad (52)$$

Finally, substituting Eq. 52 into Eq. 49, we arrive at the result of Eq. 30 corresponding to Fig. 12.

For the regime II we have in a similar way:

$$F(\sigma) \approx \sigma(\tau + \sigma/2), \quad \sigma(F) \approx \sqrt{2F + \tau^2} - \tau, \quad (53)$$

$$\varphi(F) \approx \frac{2}{3} \left[(2F + \tau^2)^{3/2} - \tau(3F + \tau^2) \right], \quad F(\xi) \approx \left[F_0^{1/4} - \lambda_1 \xi + \frac{3\tau}{2^{5/4} (F_0^{1/4} - \lambda_1 \xi)} \right]^4,$$

with $\lambda_1 = 2^{1/4}k/(4\sqrt{3})$, obtaining the charge density distribution (Fig. 13e):

$$\sigma(\xi) \approx (\sqrt{\sigma_0 + \tau} - \lambda_1 \xi)^2 - \tau. \quad (54)$$

This function seems to turn zero already at $\xi = (\sqrt{\sigma_0 + \tau} - \sqrt{\tau})/\lambda_1$, but in fact the fast parabolic decay by Eq. 54 only extends to $\xi \sim \xi^*$, such that $\sigma(\xi^*) \sim \rho_0$, and for $\xi > \xi^*$ the decay turns exponential, like Eq. 30. The I - V characteristics, Eq. 33, follows directly from Eq. 54.

References

- [1] A.E. Berkowitz, J.R. Mitchell, M.J. Carey, A.P. Young, S. Zhang, F.T. Parker, A. Hutten, G. Thomas, Phys. Rev. Lett. **68**, 3745 (1992).
- [2] L.F. Schelp, A. Fert, F. Fettar, P. Holody, S.F. Lee, J.L. Maurice, F. Petroff, A. Vaurès, Phys. Rev. B **56**, R5747 (1997).
- [3] H. Imamura, J. Chiba, S. Mitani, K. Takanashi, S. Takahashi, S. Maekawa, H. Fujimori, cond-mat/9904272.
- [4] M.A. Parker, K.R. Coffey, J.K. Howard, C.H. Tsang, R.E. Fontana, T.L. Hylton, IEEE Trans. Magn. **32**, 142 (1996).
- [5] B. Dieny, S. Sankar, M.R. McCartney, D.J. Smith, P. Bayle-Guillemaud, A.E. Berkowitz, J. Magn. Magn. Mater. **185**, 283 (1998).

- [6] G.N. Kakazei, A.M.L. Lopes, Yu.G. Pogorelov, J.A.M. Santos, J.B. Sousa, P.P. Freitas, S. Cardoso, E. Snoeck, J. Appl. Phys. **87**, 6328 (2000).
- [7] D. M. Schaadt, E.T. Yu, S. Sankar, A.E. Berkowitz, Appl. Phys. Lett. **74**, 472 (1999).
- [8] P. Sheng, B. Abeles . Phys. Rev. Lett. **28**, 34 (1972).

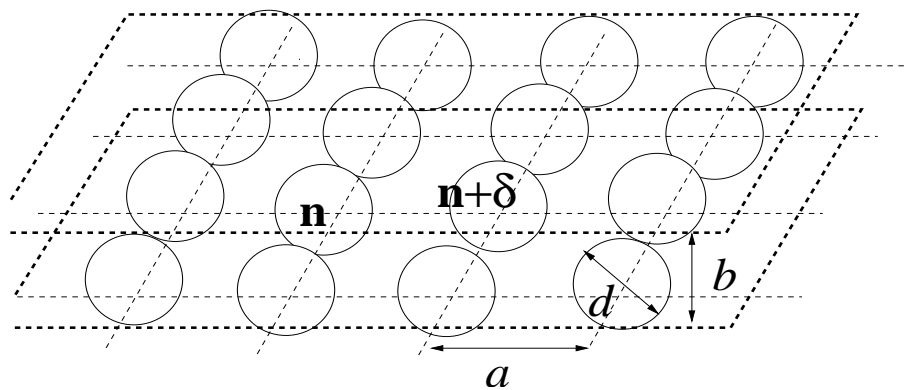


Fig.1: Square lattice of granules in insulating matrix.

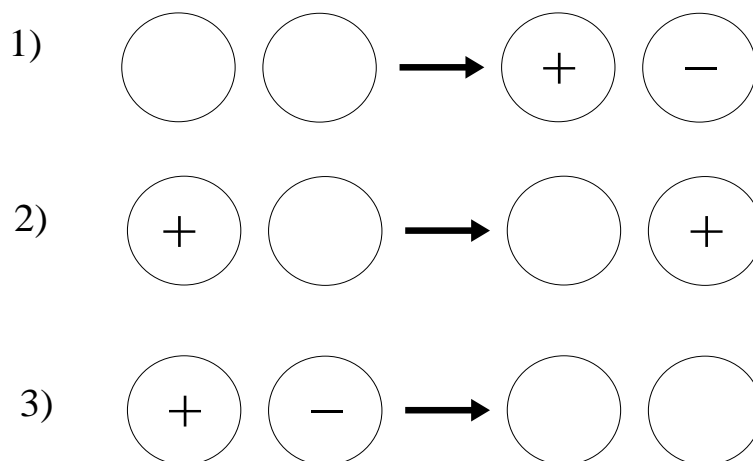


Fig.2: Kinetic processes in a granular layer.

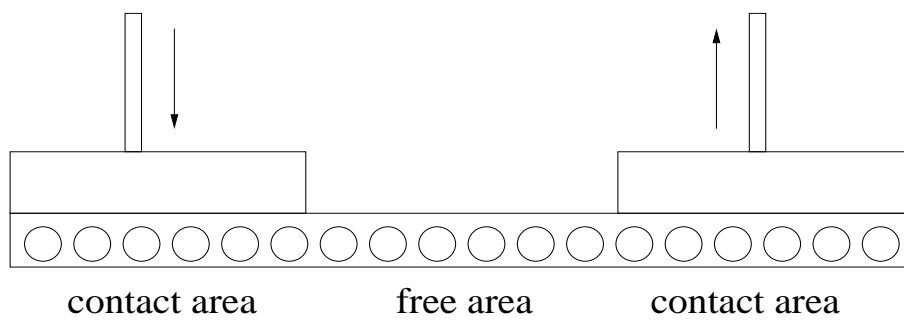


Fig.3: CIP conduction geometry.

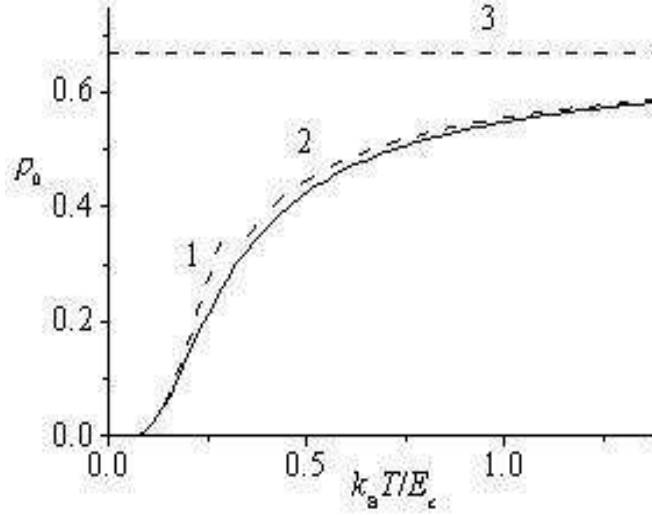


Fig.4: Equilibrium density ρ_0 of charge carriers in function of temperature (solid line). The curve 1 (dashed line) corresponds to low temperature asymptotics $\rho_0 \approx 2 \exp(-E_c/2k_B T)$, and the curve 2 (dash-dotted-line) to high temperature asymptotics $\rho_0 \approx \rho_\infty - E_c/9k_B T$, converging to the limit $\rho_\infty = \frac{2}{3}$.

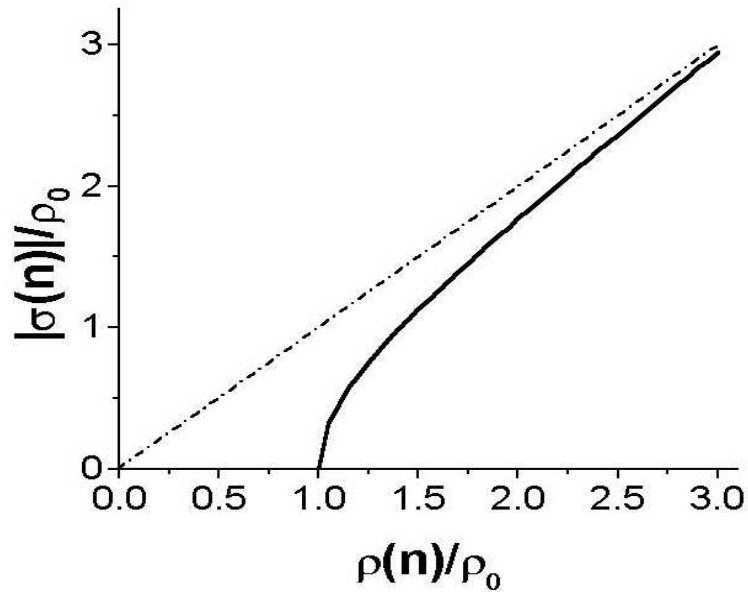


Fig.5: Relation between local charge density σ and charge carrier density ρ (both normalized to the thermal equilibrium value ρ_0).

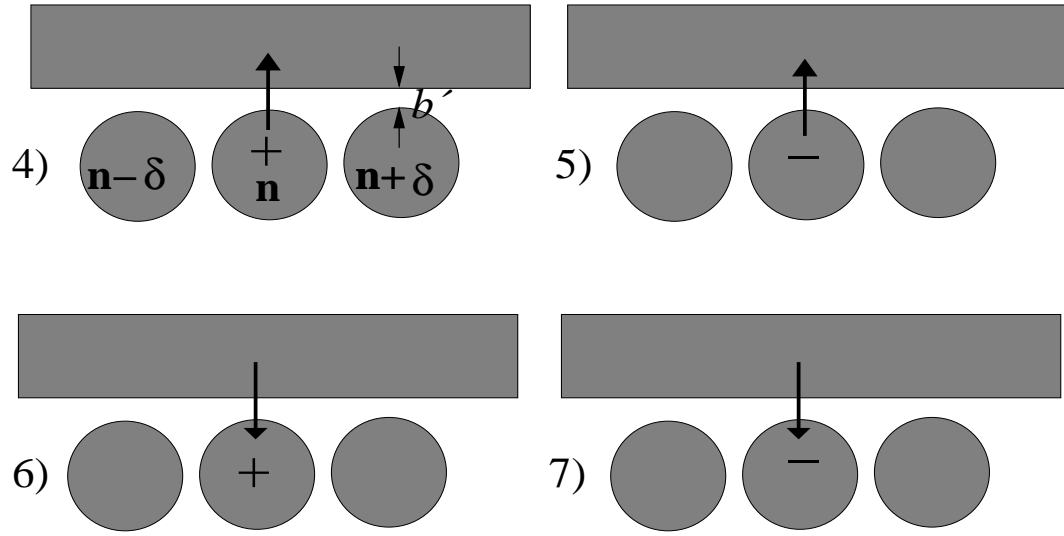


Fig.6: Kinetic processes between n th granule and metallic electrode in CA.

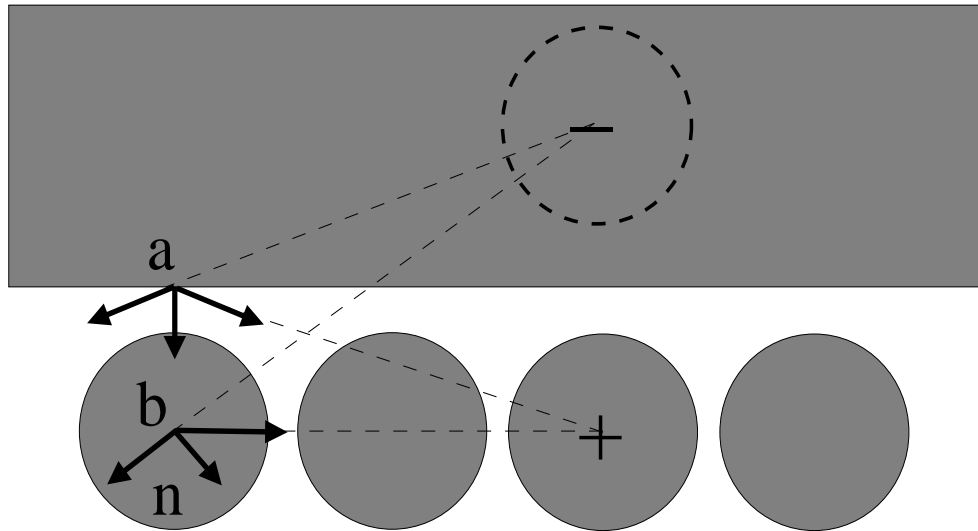


Fig.7: Formation of local electric field by charged granules and their images at the surface of metallic electrode (point a) and between the granules (point b).

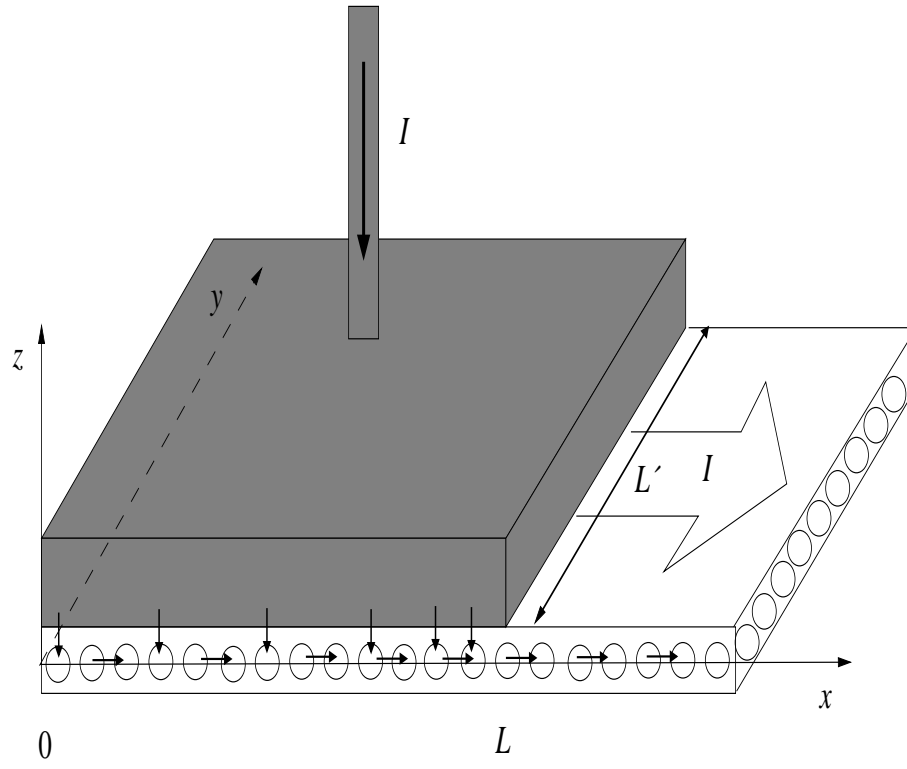


Fig.8: Relations between n th longitudinal (j_x) and normal (j_z) currents in CA.

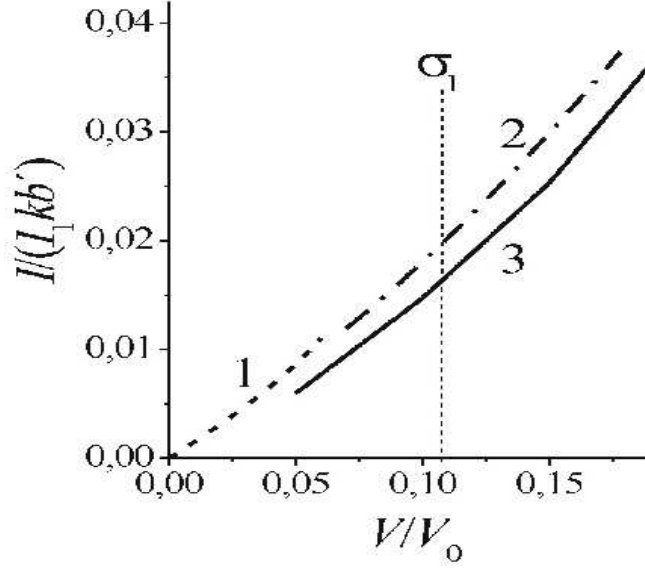


Fig.9: I-V characteristics for CA, line 1 (short dashes) for regime 1, line 2 (dash-and-dot) for regime 2, and line 3 (solid) for numeric solution of Eq. 24.

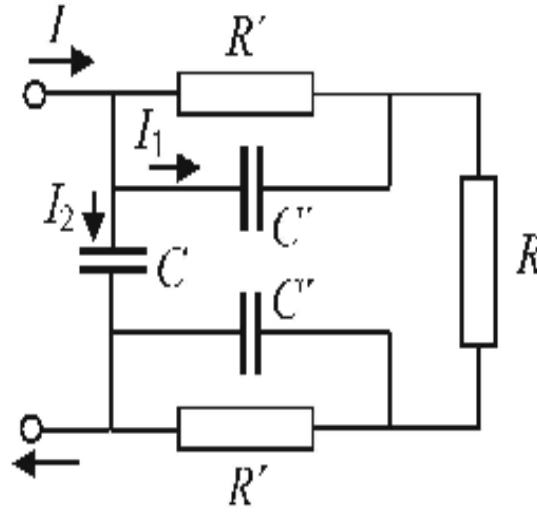


Fig.10: Equivalent circuit for transient regimes of CIP conductance.

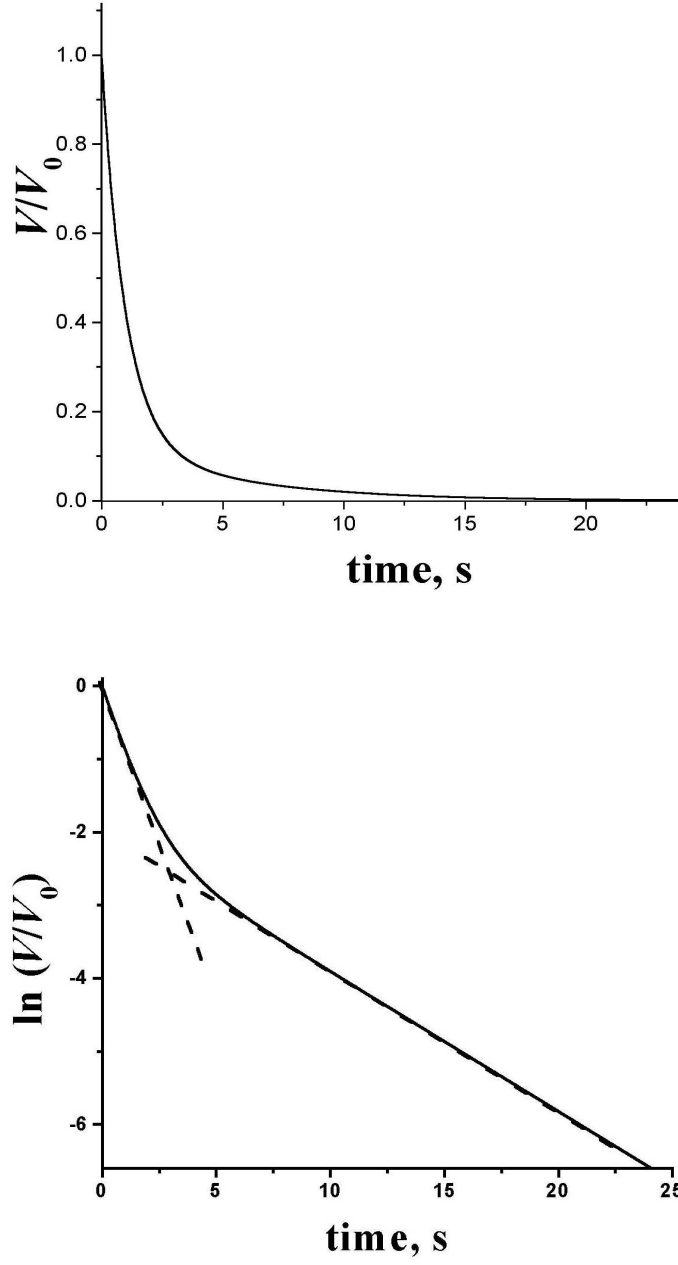


Fig.11: Charge relaxation at disconnecting the steady state circuit. Log plot (lower panel) reveals two strongly different relaxation times.

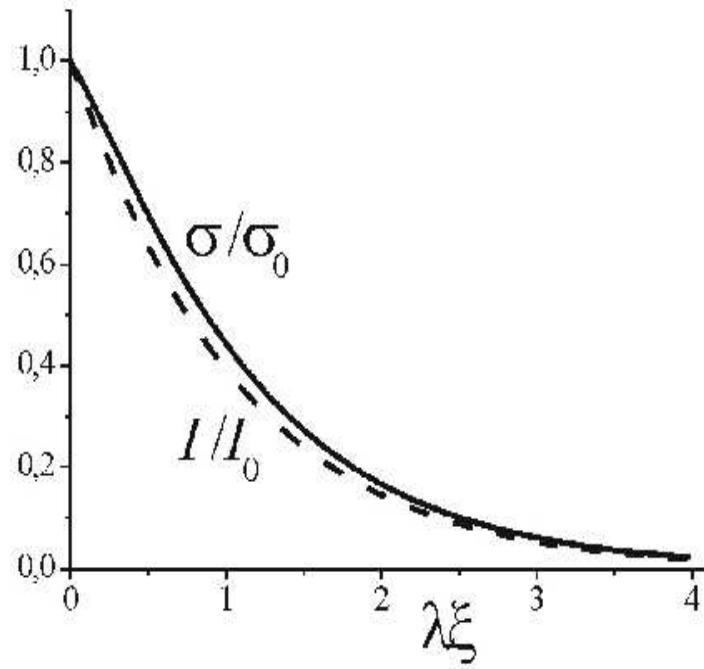


Fig.12 : Charge density and current distribution in CA(regime I).

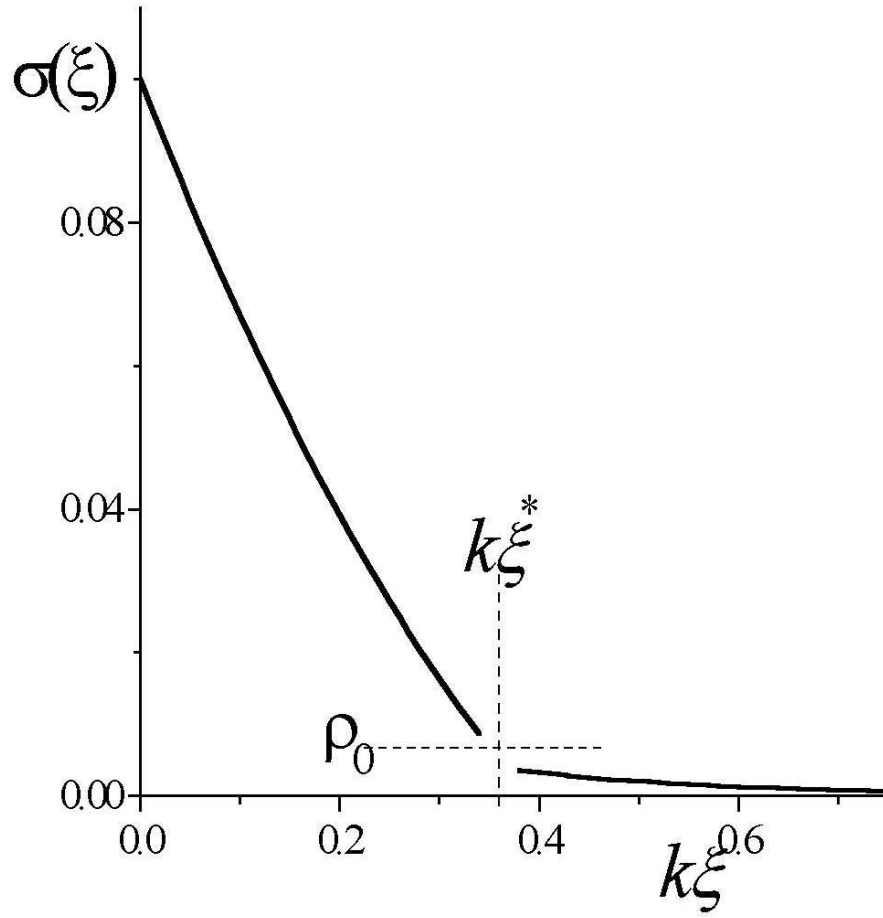


Fig.13: Charge density in regime II. A fast decay by Eq.53 is changed to a slower exponential law, Eq.29, after density dropping below the characteristic value ρ_0 .